Artificial intelligence-based CT metrics in relation with clinical outcome of COVID-19 in young and middle-aged adults

Sihui Zeng
Sun Yat-sen University Cancer Center
Weihong Liu
General hospital of China Resources & Wuhan Iron and Steel Corporation
Xudong Yu
Hubei maternal and Child Health Hospital
Yanli Li
Hubei maternal and Child Health Hospital
Jiao Gao
General hospital of China Resources & Wuhan Iron and Steel Corporation
Jiawei Li
General hospital of China Resources & Wuhan Iron and Steel Corporation
Hanhui Li
Shanghai United Imaging Intelligence Co., Ltd.
Liang Mao
Shanghai United Imaging Intelligence Co., Ltd.
Chuanmiao Xie (xiechm@sysucc.org.cn)
Sun Yat-sen University Cancer Center
Jianye Liang (ljyjnu@foxmail.com)
Sun Yat-sen University Cancer Center

Research Article

Keywords: Artificial intelligence, CT, Coronavirus, infection, Pneumonia

Posted Date: April 23rd, 2020

DOI: https://doi.org/10.21203/rs.3.rs-24561/v1

Abstract

Purposes: Currently, most researchers mainly analyzed COVID-19 pneumonia visually or qualitatively, probably somewhat time-consuming and not precise enough. This study aimed to excavate more information, such as differences in distribution, density, and severity of pneumonia lesions between males and females in a specific age group using artificial intelligence (AI)-based CT metrics. Besides, these metrics were incorporated into a clinical regression model to predict the short-term outcome.

Methods: The clinical, laboratory information and a series of HRCT images from 49 patients, aged from 20 to 50 years and confirmed with COVID-19, were collected. The volumes and percentages of infection (POI) among bilateral lungs and each bronchopulmonary segment were extracted using uAI-Discover-NCP software (version R001). The POI in three HU ranges, (i.e. <-300, -300~49 and ≥50 HU representing ground-glass opacity (GGO), mixed opacity and consolidation), were also extracted. Hospital stay was predicted with several POIs after adjusting days from illness onset to admission, leucocytes, lymphocytes, c-reactive protein, age and gender using a multiple linear regression model.

Results: Right lower lobes had the highest POI, followed by left lower lobes, right upper lobes, middle lobes and left upper lobes. The distributions in lung lobes and segments were different between the sexes. Men had a higher total POI and GGO of the lungs, but less consolidation than women in initial CT (all $p<0.05$). The total POI, percentage of consolidation on initial CT and changed POI were positively correlated with hospital stay in the model.

Conclusion: Both men and women had characteristic distributions in lung lobes and bronchopulmonary segments. AI-based CT quantitative metrics can provide more precise information regarding lesion distribution and severity to predict clinical outcome.

Introduction

Beginning in December 2019, a new pneumonia named as Coronavirus Disease 2019 (COVID-19) was initially reported in Wuhan, Hubei province and has gradually spread throughout the country. Since then, there have been more than 82,000 confirmed cases and 3,300 deaths reported in China. The epidemic in China has been well controlled, while other countries are still on the rise phase. The confirmed number has exceeded 940,000 from other countries, with more than 50,000 deaths. Since the World Health Organization announced the outbreak of COVID-19 as a Public Health Emergency of International Concern on January 30, 2020, many countries or regions have successively declared a state of emergency and upgraded their responses to the first / highest level. The disease was caused by a betacoronavirus, which was newly named severe acute respiratory syndrome coronavirus 2 (SARS-CoV-2). It has a strong infectivity from person to person. However, the clinical symptoms and disease severity varied a lot among different crowds as the pathogenicity is relatively weak, with an overall mortality of 2%.

Reverse transcription polymerase chain reaction (RT-PCR) or gene sequencing is the golden standard for the diagnosis of COVID-19. However, they have several limitations such as inadequate test kits for timely diagnosis in a large population suspected. Besides, the sensitivity is low with a total positive rate about 30% to 60% at an initial test [1]. For the high acquisition speed and accuracy in detecting pulmonary lesions, CT has been affirmed as the preferred imaging tool in diagnosing COVID-19 and recommended as the major evidence for clinically diagnosed cases in this epidemic in Hubei, China [2]. Currently, most researchers mainly analyzed COVID-19 pneumonia visually or qualitatively, which probably time-consuming and exhausting, especially in a rapidly increasing infected population and when demanded to compare with previous examinations [3]. The accuracy was low as a lot of information based on lesions volumes and density were omitted. Besides, the blurred lesion borders and low density of ground-glass opacity (GGO) will confuse radiologists when evaluating the lesion severity. Inspiringly, artificial intelligence (AI) based on deep learning technology has been attempted to diagnose COVID-19 and make a differentiation from other pneumonia, which demonstrates a great prospect for its high capability in feature extraction [4, 5]. Shan et al.[6] employed the “VB-Net” neural network to segment COVID-19 infection and a human-in-the-loop strategy to train the system for quantification of infection regions. The system generated a Dice similarity coefficient as high as 90% between automatic and manual segmentations, and a mean percentage of infection (POI) estimation error of 0.3% for the whole lung on the validation dataset, which indicated a high accuracy for automatic infection region delineation.

The occurrence and case fatality rate was revealed higher in men in a similar viral pneumonia (MERS-CoV infection) [7]. However, limited data was available about the difference between the sexes when comparing the epidemiological, clinical and imaging feature in COVID-19. Hence we employed the deep learning system to extract quantitative CT metrics to compare the difference in distribution, density, and severity of pneumonia lesions between males and females in a specific age group, to maximally eliminate the influence of age, especially in children and the elderly. Besides, these metrics were incorporated into a clinical regression model to evaluate the short-term outcome.

Materials And Methods

Patients

This study was conducted in accordance with the amended Declaration of Helsinki and had been approved by the ethics committee of *General hospital of China Resources & Wuhan Iron and Steel Corporation*. The individual consent was waived due to the retrospective nature. The clinical, laboratory and CT imaging data of patients with COVID-19 in *General hospital of China Resources & Wuhan Iron and Steel Corporation* from January 11, 2020 to March 18, 2020 were collected and analyzed retrospectively. The inclusion criteria were as follows: (1) the patients were confirmed with SARS-CoV-2 by real-time fluorescent RT-PCR or viral gene sequence; (2) the patients aged from 20 to 50 years; (3) only moderate, severe and critical cases with radiological findings of pneumonia were included, according to the Diagnosis and Treatment Protocol for Novel Coronavirus Pneumonia (Trial Version 7) [8], and (4) those who completed the initial chest CT examination within three days after the illness onset, and had at least

one follow-up CT scan within one week after the initial examination. The general clinical symptoms and laboratory results were collected, especially including white blood cell count, lymphocyte count, C-reactive protein (CRP). Exclusion criteria were: (1) patients accompanied with hypertension, diabetes, heart diseases and any other pulmonary diseases; and (2) pregnant woman.

Imaging protocol

The patients underwent the chest CT examination on a Somatom Definition AS+ 64-row scanner (Siemens Healthineers; Erlangen, Germany) and a uCT 530 40-row scanner (United Imaging Intelligence, China). The scanning parameters were set as follows: tube voltage=120 kVp, automatic tube current modulation, matrix=512×512, slice thickness=5 mm and spacing=5 mm. The volumetric data with reconstructed 0.6 to 1-mm slice thickness were obtained for post-processing.

Deep learning model

Two radiologists analyzed the CT images and collected the quantitative CT metrics. The assisted screening software for COVID-19 (United Imaging Intelligence, version R001, China) was utilized to screen lung lesions by VB-Net network and to segment lesion areas in lung window [6, 9]. Figure 1 showed the interface and function of this software. After segmentation, various indicators were calculated to quantify lung infections, including the volumes of infection in the entire lung, as well as each lobe and each bronchial lung segment. In addition, POI was calculated for the entire lung, each lobe, and bronchopulmonary segment to measure the severity of COVID-19 and the distribution of intra-pulmonary infections. The POI in three HU ranges, (i.e. <-300, -300~49 and ≥50 HU representing ground-glass opacity (GGO), mixed opacity and consolidation), were also extracted [10]. ΔPOI was defined as the difference value of total POI in whole lungs between the second CT and initial CT scans. For clinical purpose, the principle of the AI system was not further illustrated in this study.

Statistical analysis

SPSS 13.0 software (IBM Corporation, Chicago, IL, USA) and GraphPad Prism 5.01 (GraphPad Software Inc., San Diego, CA) were used to perform statistical tests and plot bar charts. Kolmogorov-Smirnov test was used to assess the data distribution type. The numeric results are presented as the mean ± standard deviation (SD). Independent sample t test for continuous variables, and χ^2 or Fisher exact test for categorical variables was used to compare the difference between the sexes. A multiple linear regression model was used to explore the values of initial total POI (iPOI), ΔPOI and percentage of consolidation in evaluating the hospital stay, after adjusting days from illness onset to admission, leucocytes, lymphocytes, c-reactive protein (CRP), age and gender (male=1 and female=0). A P-value < 0.05 was considered statistically significant.

Results

Clinical and Laboratory Findings

The basic clinical and laboratory information were listed in table 1. There were 21 men and 28 women with 147 examinations included for analysis. All the patients had at least two CT scans, 14 patients had four, and 29 had three for comparisons. Men had lower PaO_2 (P=0.002) and shorter days from illness onset to admission (P=0.001) than women. Men also had a longer hospital stay (15.9±7.9 vs 14.6±5.2, P=0.507) and higher proportion of severe and critical cases than women (52.4% vs 32.1%, P=0.387). However, the results were insignificant. No significant difference was observed between the sexes in age, heart rate, respiratory rate, fever, cough, headache, myalgia and sore throat (all P>0.05), except fatigue (P=0.038). More than half of men and women showed decreased leucocytes and lymphocytes counts as well as increased CRP, but without significant difference between them.

Artificial intelligence-based CT features

The correlations between CT metrics, clinical and laboratory indicators were listed in Table 2. Figure 2 showed a COVID-19 patient with disease remission in a coronal and three-dimensional view with lesions highlighted. Figure 3 showed a COVID-19 patient with disease progression in the same view. Initial infection distribution in each lung lobe and bronchopulmonary segment in a total population, and in men and women were plotted in Figure 4. Overall, right lower lobes had the highest POI, followed by left lower lobes, right upper lobes, middle lobes and left upper lobes. The distributions of infections in lung lobes and bronchopulmonary segments were different between men and women. Men had higher POIs in entire lungs (t=2.105, P=0.041), left (t=2.291, P=0.026) and right upper lobes (t=2.521, P=0.015), and right middle lobes (t=2.231, P=0.031), but lower POIs in left (t=-1.669, P=0.102) and right lower lobes (t=-0.879, P=0.384). Moreover, regarding the bronchopulmonary segment level, men had significantly higher POIs in apicoposterior segment (t=2.075, P=0.044), anterior segment (t=2.038, P=0.047), superior lingular segment (t=2.431, P=0.019), but lower POIs in dorsal segment (t=-2.148, P=0.037), lateral basal segment (t=-2.033, P=0.048), and posterior basal segment (t=-2.639, P=0.011) of left lung. Higher POIs in apical segment (t=2.287, P=0.029), posterior segment (t=2.235, P=0.030), anterior segment (t=2.428, P=.021), lateral segment (t=2.129, P=0.039), and medial segment (t=2.103, P=0.046), and lower POIs in lateral basal segment (t=-2.333, P=0.024) and posterior basal segment (t=-2.285, P=0.027) of right lung were also observed in men. These results indicated that the lesions were more likely to occur in or extend to bilateral upper lobes, superior lingular segment and right middle lobes in men, which were more close to upper and front sides. The lesions in women were more concentrated in bilateral lower lobes, especially in dorsal segment, lateral basal segment and posterior basal segment, which were more close to outer and back sides.

Figure 4D plotted the percentages of three components on initial and follow-up CTs among men and women. From above results, men showed a higher total POI and extensive infection while women showed a less proportion but more intensive infection, prompting us that whether there existed a difference in the lesion density. After segmentation and quantitatively calculating the percentages of GGO, mixed opacity and consolidation based on CT values, men had higher percentages of GGO (t=2.227, P=0.031), but less mixed opacity (t=-0.465, P=0.644) and consolidation (t=-2.113, P=0.040) than women in initial CT, conforming our hypothesis. From Figure 4D, we found that the percentage of GGO reached a peak on the

second CT in both men and women, while the percentage of mixed opacity and consolidation maintained a high platform. Afterwards, the components started to decrease, and obviously on the fourth CT.

Quantitative CT metrics in regression model

In this part, we hypothesize that the duration of hospital stay could reflect the severity of illness and probably correlate with some of laboratory and imaging indicators. Therefore, a linear regression model was established and evaluated for the values of iPOI, ΔPOI and percentage of consolidation in relation with the short-term outcome. The correlations between the three CT metrics and clinical as well as laboratory indicators were listed in Table 2. The unstandardized and standardized coefficients among each independent variable and dependent variable, as well as the collinearity statistics were listed in Table 3. Overall, R=0.928 indicated a high model-fitting degree and adjusted R^2=0.830 suggested all these independent variables collectively contributed the major variations in hospital stay. The Durbin-Watson coefficient was 1.984, which was close to 2. All the Tolerance coefficients were larger than 0.1 and variance inflation factors were less than 10, indicating that there was no multicollinearity among these independent variables. Their Standardized β were compared and suggested that CRP, percentage of consolidation, iPOI, ΔPOI and lymphocyte counts degressively contributed to hospital stay. In this model, no correlation was found between days from illness onset to admission, leucocyte counts, age, gender and hospital stays. The model indicates a larger percentage of infection and more consolidation components on initial CT, and an obvious increase of POI on follow-up CT will significantly prolong the duration of hospital stay. Besides, the iPOI, ΔPOI and percentage of consolidation showed mild to moderate correlations with CRP, leucocytes and lymphocyte counts (Pearson correlation coefficients ranged from 0.381 to 0.608, but less than 0.7).

Discussion

Currently, CT imaging plays an important role in screening COVID-19 and evaluating the severity of illness in the pandemic of viral pneumonia. A tool that can automatically quantify the lesions characteristics will significantly improve the work efficiency and diagnostic accuracy. Deep learning has become a promising technique in medical image analysis for feature extraction, and successfully been applied to analyze diffuse interstitial lung disease [11] and differentiate viral and bacterial pneumonia on chest radiographs or CT images [4, 12]. In this study, we used a deep learning-based software to segment and quantify the volume and percentage of COVID-19 infection on three-dimensional CT volumetric images, which help us excavate more detailed information regarding lesion distribution, density, and the progress of each component on follow-up CT between the sexes.

In this study, we found that men had a longer duration of hospital stay, higher proportion of severe and critical cases and lower PaO_2 than women. Initial CT also suggested that men had a higher iPOI in entire lungs than women. Though only PaO_2 and iPOI showed statistical difference, they can still prompt that men may showed a higher degree of severity when infected with SARS-CoV-2. A rapid progress was also observed in men regarding the shorter days from illness onset to admission and significantly higher ΔPOI

(10.1% vs 7.6%), compared with women. Many studies had reported the relationship between estrogen and immune system in antiviral response. One study had indicated that the diffuse alveolar damage in severe influenza was correlated with excessive inflammation, while estradiol was an effective anti-inflammatory hormone that relieved the severity of influenza A virus infection in women [13]. It can recruit more neutrophils to improve the reaction of influenza virus-specific $CD8^+$ T cells for releasing more IFN-γ and TNF-α. They can promote virus elimination and improve the clinical outcome [14]. Another study also indicated that a higher level of testosterone may suppress their immune response and caused a higher morbidity of influenza in men [15]. Our study subdivided and quantified the contents of three components, and tracked their follow-up changes, which may also reflect the dynamic process of pathology. GGO was a feature of alveolar edema and exudation of acute pulmonary injury while consolidation suggested that the alveolus was completely filled with dense inflammatory exudation [16]. We found that men had more extensive and larger volume of GGO in bilateral lungs while women showed less volume but denser lesions in bilateral lower lobes. Estrogen may help the immune system detect and confront the virus in an early stage [13], which could restrict the infection within the originally preferred regions. Regarding a larger percentage of consolidation in women on initial CT, the lesions may progress into a relatively late stage due to the longer days from illness onset to admission, compared to men. However, except for fatigue, the initial clinical symptoms were not showing difference between the sexes, indicating that this may not be the factor that influence the clinical outcome.

In the regression model, we incorporated iPOI and percentage of consolidation simultaneously into the model, considering that consolidation can reflect the severity of lesions in term of lesion density but only accounts for a small proportion in total infection. Change in percentage of consolidation will not obviously improve iPOI. Besides, no multiple collinearity was observed between any other two independent variables in this model. We found that the duration of hospital stay was positively correlated with iPOI, ΔPOI, percentage of consolidation and CRP, and negatively correlated with lymphocyte count. Guan et al.[17] had already reported that severe cases of COVID-19 showed significantly higher amounts of CRP than non-severe cases. A previous study showed that CT-based pulmonary inflammation index correlated with lymphocytes count, monocyte count, CRP and procalcitonin, but correlation strengths were quite low with correlation coefficients ranging from 0.258 to 0.373 due to a semiquantitative value used [16]. In our study, a more precise quantifying technique was introduced and the iPOI, ΔPOI, and percentage of consolidation showed higher correlations with leucocyte, lymphocyte counts and CRP with the coefficients ranged from 0.381 to 0.608. Besides, the three CT metrics contributed the major variations (83%) in hospital stay combined with laboratory indicators. Though there is still no specific medicine treating to COVID-19, proper supportive treatment also help reducing the duration of hospital stay in a certain extent, and may account for the remaining part of variations in hospital stay.

There are several limitations in this study. First, the sample size is still small, which may lead to insignificant results regarding the severity of infection between the sexes, largely because we set strict inclusion criteria to maximally eliminate the influence of age and accompanied diseases, and include the patients with more follow-up CT to track the dynamic changes of COVID-19. Second, the other laboratory

indicators (e.g. neutrophil count, procalcitonin and D-Dimer) and imaging features (e.g. pleural effusion and lymphadenectasis) which may correlate with the clinical outcome were not investigated. Though the POIs within any HU intervals could be precisely extracted, the ideal threshold with the best diagnostic performance to distinguish GGO or mixed opacity from consolidation was still unclear.

Conclusion

In this study, we used a more precise analyzing method to confirm the predilection of lesion distribution and severity of COVID-19 among men and women in a more homogeneous age group. Both men and women had characteristic distributions in lung lobes and bronchopulmonary segments. AI-based CT metrics can improve the recognition and quantification of GGO, mixed density and consolidation, and help the radiologists effectively and accurately determine the severity of the disease, compare the follow-up changes, and evaluate the clinical outcome. At last, men had a higher total POI and GGO of the lungs but less consolidation on initial CT, and a rapid progress on follow-up CT compared to women, which demonstrate more serious infection with relatively worse situation in men, but more patients should be included for analysis in the future.

Abbreviations

AI, artificial intelligence; COVID-19, Coronavirus Disease 2019; CT, computed tomography; CRP, C-reactive protein; GGO, ground-glass opacity; POI, percentage of infection; RT-PCR, reverse transcription polymerase chain reaction; SARS-CoV-2, severe acute respiratory syndrome coronavirus 2.

Declarations

Ethics approval /consent to participate

The study was conducted in accordance with the principles of the Declaration of Helsinki. Approval was granted by the Ethics Committee of General hospital of China Resources & Wuhan Iron and Steel Corporation. The written informed consent for this retrospective study was waived.

Conflict of interest

The authors have stated explicitly that there are no conflicts of interest in connection with this article.

Funding

Not applicable

Data availability

The original data will be provided if requested to the corresponding authors.

Author contributions

LJY, XCM and ZSH conceived the study and revised the manuscript. LWH, GJ and LJW acquired the data and authored the manuscript. YXD and LYL performed data analysis and interpretation. LHH and ML developed the artificial intelligence system. All authors contributed substantially to the writing and review of the manuscript.

Acknowledgments: None

References

1. Ai T, Yang Z, Hou H, Zhan C, Chen C, Lv W, Tao Q, Sun Z, Xia L: Correlation of Chest CT and RT-PCR Testing in Coronavirus Disease 2019 (COVID-19) in China: A Report of 1014 Cases. *Radiology* 2020:200642. doi:10.1148/radiol.2020200642
2. Zu ZY, Jiang MD, Xu PP, Chen W, Ni QQ, Lu GM, Zhang LJ: Coronavirus Disease 2019 (COVID-19): A Perspective from China. *Radiology* 2020:200490. doi:10.1148/radiol.2020200490
3. Xu X, Yu C, Qu J, Zhang L, Jiang S, Huang D, Chen B, Zhang Z, Guan W, Ling Z *et al*: Imaging and clinical features of patients with 2019 novel coronavirus SARS-CoV-2. *Eur J Nucl Med Mol Imaging* 2020:In press. doi:10.1007/s00259-020-04735-9
4. Li L, Qin L, Xu Z, Yin Y, Wang X, Kong B, Bai J, Lu Y, Fang Z, Song Q *et al*: Artificial Intelligence Distinguishes COVID-19 from Community Acquired Pneumonia on Chest CT. *Radiology* 2020:200905. doi:10.1148/radiol.2020200905
5. Li D, Wang D, Dong J, Wang N, Huang H, Xu H, Xia C: False-Negative Results of Real-Time Reverse-Transcriptase Polymerase Chain Reaction for Severe Acute Respiratory Syndrome Coronavirus 2: Role of Deep-Learning-Based CT Diagnosis and Insights from Two Cases. *Korean J Radiol* 2020, 21(4):505-508. doi:10.3348/kjr.2020.0146
6. Shan F, Gao Y, Wang J, Shi W, Shi N, Han M, Xue Z, Shi Y: Lung Infection Quantification of COVID-19 in CT Images with Deep Learning. 2020:https://arxiv.org/abs/2003.04655.
7. Alghamdi IG, Hussain, II, Almalki SS, Alghamdi MS, Alghamdi MM, El-Sheemy MA: The pattern of Middle East respiratory syndrome coronavirus in Saudi Arabia: a descriptive epidemiological analysis of data from the Saudi Ministry of Health. *Int J Gen Med* 2014, 7:417-423. doi:10.2147/IJGM.S67061
8. National Health Commission & State Administration of Traditional Chinese Medicine: Diagnosis and Treatment Protocol for Novel Coronavirus Pneumonia (Trial Version 7). 2020:http://www.healthcare-assoc.org/.
9. Mu G, Lin Z, Han M, Yao G, Gao Y: Segmentation of kidney tumor by multi-resolution VB-nets. 2019:DOI: 10.24926/548719.548003. Https://www.researchgate.net/publication/336247962_Segmentation_of_kidney_tumor_by_multi-resolution_VB-nets.

10. Scholten ET, Jacobs C, van Ginneken B, van Riel S, Vliegenthart R, Oudkerk M, de Koning HJ, Horeweg N, Prokop M, Gietema HA *et al*: Detection and quantification of the solid component in pulmonary subsolid nodules by semiautomatic segmentation. *Eur Radiol* 2015, 25(2):488-496. doi:10.1007/s00330-014-3427-z
11. Park B, Park H, Lee SM, Seo JB, Kim N: Lung Segmentation on HRCT and Volumetric CT for Diffuse Interstitial Lung Disease Using Deep Convolutional Neural Networks. *J Digit Imaging* 2019, 32(6):1019-1026. doi:10.1007/s10278-019-00254-8
12. Kermany DS, Goldbaum M, Cai W, Valentim CCS, Liang H, Baxter SL, McKeown A, Yang G, Wu X, Yan F *et al*: Identifying Medical Diagnoses and Treatable Diseases by Image-Based Deep Learning. *Cell* 2018, 172(5):1122-1131 e1129. doi:10.1016/j.cell.2018.02.010
13. Vermillion MS, Ursin RL, Attreed SE, Klein SL: Estriol Reduces Pulmonary Immune Cell Recruitment and Inflammation to Protect Female Mice From Severe Influenza. *Endocrinology* 2018, 159(9):3306-3320. doi:10.1210/en.2018-00486
14. Robinson DP, Hall OJ, Nilles TL, Bream JH, Klein SL: 17beta-estradiol protects females against influenza by recruiting neutrophils and increasing virus-specific CD8 T cell responses in the lungs. *J Virol* 2014, 88(9):4711-4720. doi:10.1128/JVI.02081-13
15. Furman D, Hejblum BP, Simon N, Jojic V, Dekker CL, Thiebaut R, Tibshirani RJ, Davis MM: Systems analysis of sex differences reveals an immunosuppressive role for testosterone in the response to influenza vaccination. *Proc Natl Acad Sci U S A* 2014, 111(2):869-874. doi:10.1073/pnas.1321060111
16. Wu J, Wu X, Zeng W, Guo D, Fang Z, Chen L, Huang H, Li C: Chest CT Findings in Patients with Corona Virus Disease 2019 and its Relationship with Clinical Features. *Invest Radiol* 2020:In press. doi:10.1097/RLI.0000000000000670
17. Guan WJ, Ni ZY, Hu Y, Liang WH, Ou CQ, He JX, Liu L, Shan H, Lei CL, Hui DSC *et al*: Clinical Characteristics of Coronavirus Disease 2019 in China. *N Engl J Med* 2020:In press. doi:10.1056/NEJMoa2002032

Tables

Table 1. **Basic clinical and laboratory information**

Basic information	Males (n=21)	Females (n=28)	Statistics	P value
Age (years)	39.4±7.1	42.1±5.7	-1.461	0.151
Heart rate (bpm)	100.9±15.1	98.1±14.8	0.641	0.525
Respiratory rate (breaths/min)	21.0±2.0	19.6±3.2	1.864	0.069
PaO_2 (mmHg)	93.3±3.9	96.9±3.8	-3.240	**0.002**
Days from illness onset to admission	3.0±1.3	5.4±2.0	-4.748	**0.001**
Hospital stay	15.9±7.9	14.6±5.2	0.670	0.507
Severity				
Moderate cases	10 (47.6%)	19 (67.9%)	-	0.387
Severe cases	8 (38.1%)	7 (25.0%)		
Critical cases	3 (14.3%)	2 (7.1%)		
Signs and symptoms				
Fever	18 (85.7%)	21 (75.0%)	0.317	0.574
Cough	12 (57.1%)	19 (67.9%)	0.593	0.441
Fatigue	13 (61.9%)	9 (32.1%)	4.296	**0.038**
Headache	2 (9.5%)	4 (14.3%)	-	0.688
Myalgia	10 (47.6%)	7 (25.0%)	2.710	0.100
Sore throat	12 (57.1%)	10 (35.7%)	2.227	0.136
Laboratory findings				
Leucocytes	4.4±1.7	3.9±1.8	0.877	0.385
Normal (4-10×10^9/L)	10 (47.6%)	9 (32.1%)	1.211	0.376
Decreased	11 (52.4%)	19 (67.9%)		
Lymphocytes	1.39±0.92	1.18±0.67	0.902	0.372
Normal (1.1-3.2×10^9/L)	9 (42.9%)	13 (46.4%)	0.062	0.804
Decreased	12 (57.1%)	15 (53.6%)		
C-reactive protein	23.8±20.0	21.6±17.8	0.395	0.695
Normal (<10mg/L)	7 (33.3%)	10 (35.7%)	0.030	0.862
Increased	14 (66.7%)	18 (64.3%)		

Independent sample t test for continuous variables (mean±SD), and χ^2 or Fisher exact test for categorical variables was used.

Table 2. **The correlations between CT metrics, clinical and laboratory indicators.**

Hospital stay	Days from illness onset to admission	Leucocytes	Lymphocytes	CRP	Age	Gender
0.666 (0.001)	0.118 (0.209)	**-0.456 (0.001)**	**-0.398 (0.002)**	**0.573 (0.001)**	**0.276 (0.027)**	-0.029 (0.421)
0.704 (0.001)	0.063 (0.332)	**-0.468 (0.001)**	**-0.435 (0.001)**	**0.608 (0.001)**	0.067 (0.325)	0.137 (0.175)
0.726 (0.001)	0.067 (0.324)	**-0.381 (0.003)**	**-0.437 (0.001)**	**0.594 (0.001)**	0.051 (0.363)	0.108 (0.229)

The data presented was Pearson coefficient with P value in bracket. CRP, C-reactive protein; POI, percentage of infection; ΔPOI, **the difference value of total POI in whole lungs between the second CT and initial CT scans.**

Table 3. **The unstandardized B, standardized β and collinearity statistics for each independent variable.**

	Unstandardized B	Standardized β	t	P	Collinearity Statistics	
					Tolerance	VIF
	9.8	-	3.195	0.003		
	0.129	0.212	2.703	**0.010**	0.576	1.735
	0.135	0.196	2.445	**0.019**	0.551	1.815
	1.484	0.251	3.206	**0.003**	0.576	1.737
s onset to admission	-0.029	-0.009	-0.120	0.905	0.601	1.664
	-0.580	-0.015	-0.179	0.859	0.479	2.088
	-1.607	-0.196	-2.209	**0.033**	0.450	2.220
	0.105	0.302	2.796	**0.008**	0.303	3.300
	0.015	0.015	0.219	0.828	0.723	1.383
	0.819	0.063	0.817	0.419	0.588	1.700

CRP, C-reactive protein; POI, percentage of infection; ΔPOI, **the difference value of total POI in whole lungs between the second CT and initial CT scans. VIF, variance inflation factor.**

Figures

Figure 1

Figure 1. An interface and the function of artificial intelligence–based software. The lesions were automatically delineated and segmented to calculate the infection volumes and percentages of infection in the whole lungs, lobes, bronchopulmonary segments and even within a specific HU interval.

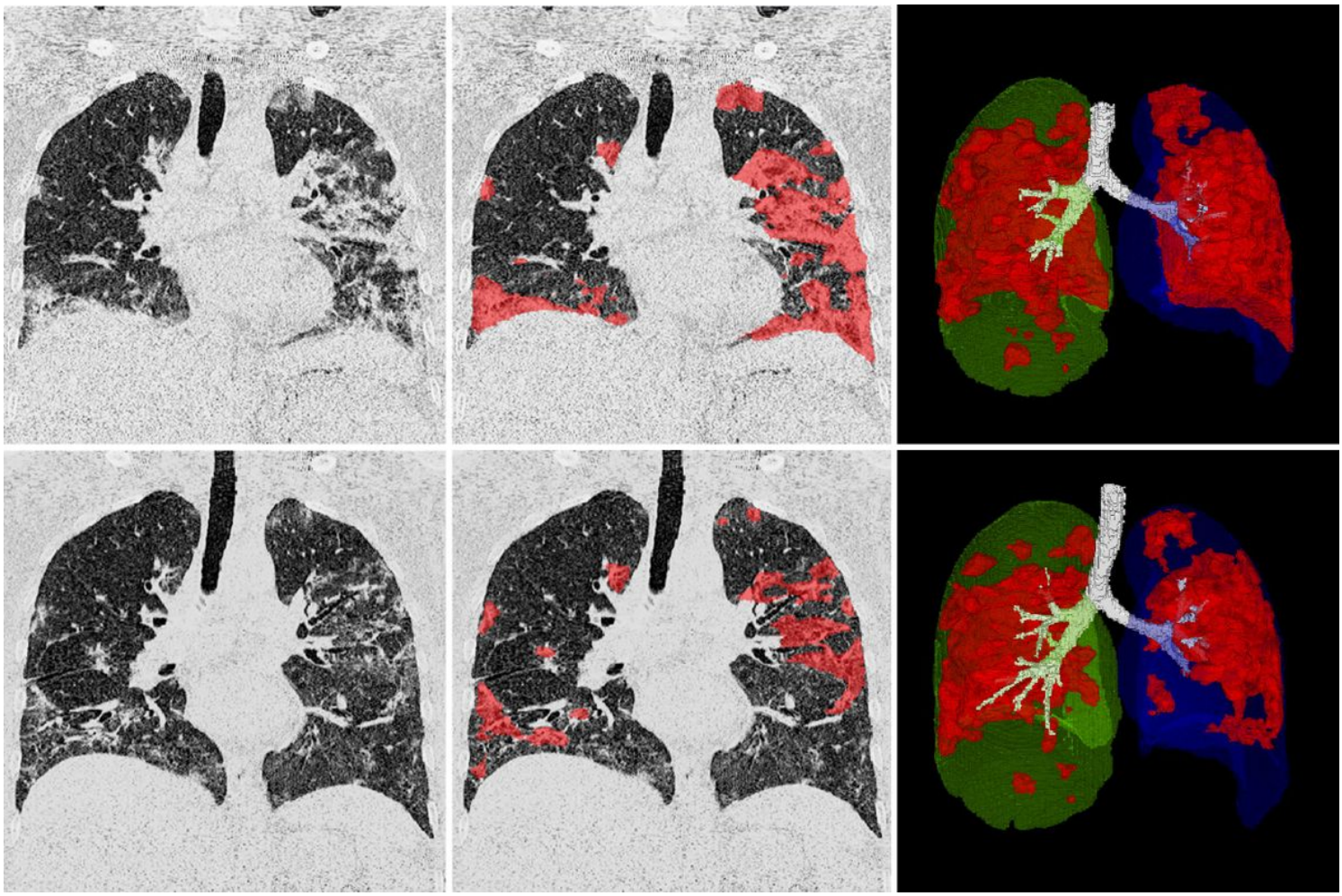

Figure 2

Figure 2. A COVID-19 patient with disease remission. Upper row and lower row showed initial and follow-up CT with standard coronal image, coronal image with color covering the lesions and 3D surface rendering image. Initial CT images showed scattered consolidations with unclear edges and irregular shapes in bilateral lungs, especially in the left lower lobe. Most lesions were absorbed and the density decreased to ground-glass opacity and mixed opacity on follow-up CT. The 3D images provided a more stereoscopic vision for comparison.

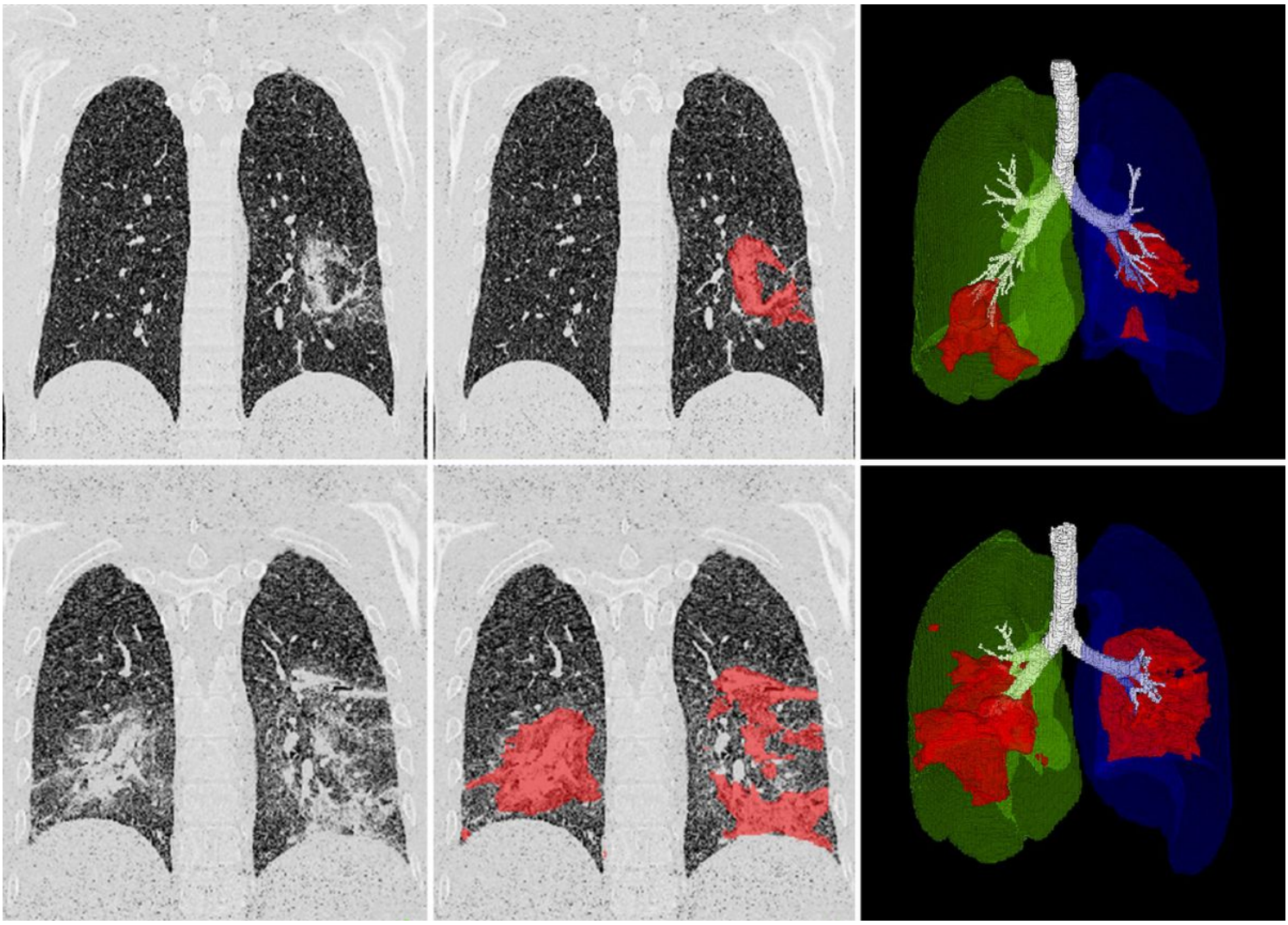

Figure 3

Figure 3. A COVID-19 patient with disease progression. Upper row and lower row showed initial and follow-up CT with standard coronal image, coronal image with color covering the lesions and 3D surface rendering image. A regional lesion was observed in the dorsal segment of left lower lobe. Both consolidation and ground-glass opacity were automatically detected and labeled with color red. The disease progress rapidly with a large area of consolidation in bilateral lower lobes observed. The lesion size in 3D image seemed to be larger than that in coronal image.

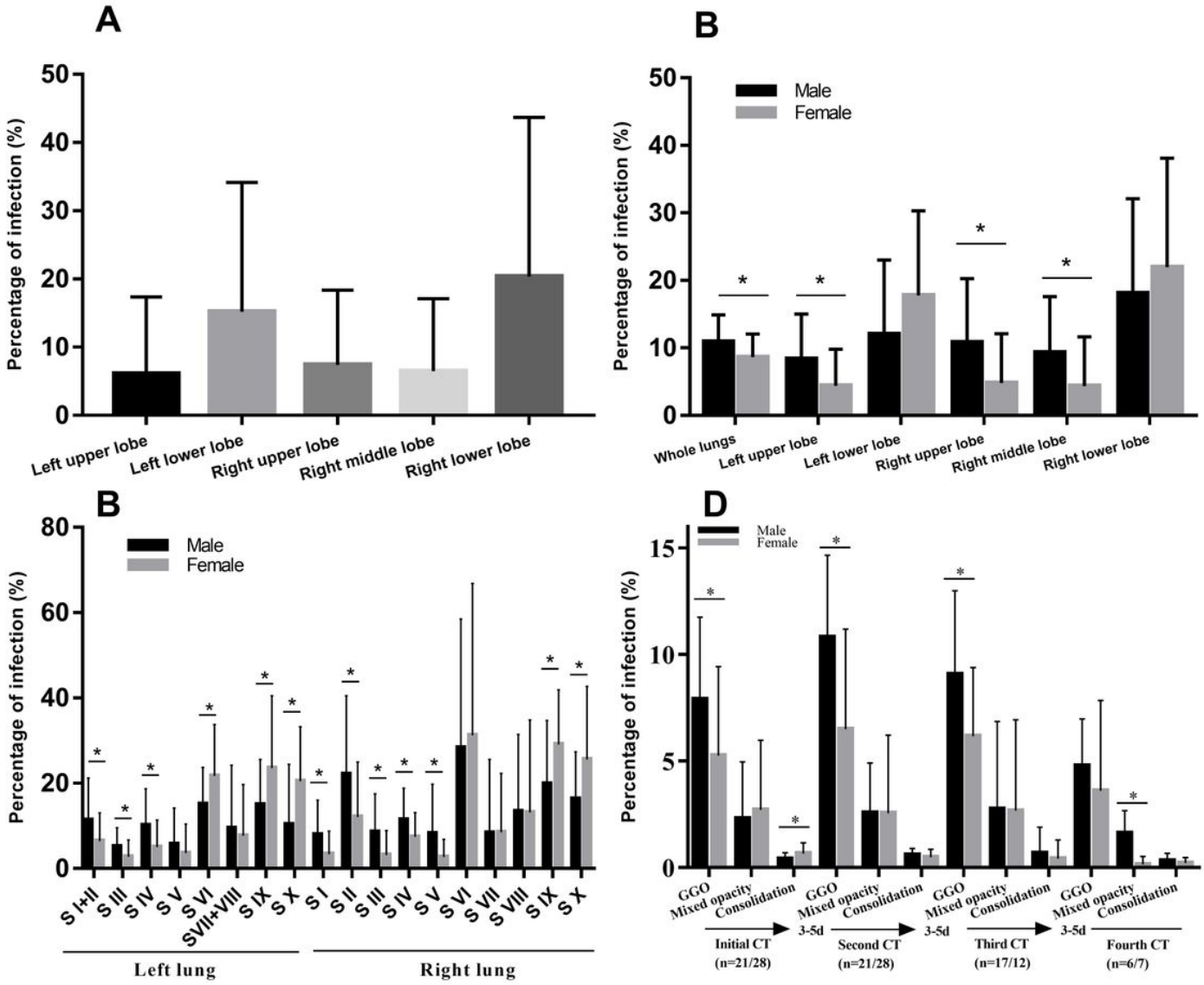

Figure 4

Figure 4. Bar charts plotted the distribution of infection in men and women. Picture A showed the overall percentage of infection (POI) in each lobe. Picture B showed the POIs in each lobe among men and women. Picture C showed the POIs in each bronchopulmonary segment among men and women. Picture D showed multiple follow-up POIs in three specific HU regions among men and women. Independent sample t test was used. *P < 0.05. Left/right upper lobe: S I, Apical segment; S II, Posterior segment; S III, Anterior segment; S I+II, Apicoposterior segment. Left upper lobe: S IV, Superior lingular segment; S V, Inferior lingular segment. Right Middle lobe: S IV, Lateral segment; S V, Medial segment. Left/right lower lobe: S VI, dorsal segment; S VII, Medial basal segment; S VIII, Anterior basal segment; S IX, Lateral basal segment; S X, Posterior basal segment; S VII+ VIII, Anterior medial basal segment.